Nighttime ionospheric *D* region parameters from VLF phase and amplitude

Neil R. Thomson,[1] Mark A. Clilverd,[2] and Wayne M. McRae[3]

Received 12 January 2007; revised 21 March 2007; accepted 12 April 2007; published 14 July 2007.

[1] Nighttime ionospheric *D* region heights and electron densities are determined from an extensive set of VLF radio phase and amplitude observations. The *D* region parameters are characterized by the traditional H' (height in kilometers) and β (sharpness in km^{-1}) as used by Wait and by the U. S. Navy in their Earth-ionosphere waveguide programs. The VLF measurements were made with several frequencies in the range 10 kHz to 41 kHz on long, mainly all-sea paths, including Omega La Reunion and Omega Argentina to Dunedin, New Zealand, NAU (Puerto Rico) and NAA (Maine, USA) to Cambridge, UK, and NPM (Hawaii) to San Francisco. Because daytime VLF propagation on such paths is readily measured and predicted, the differences between night and day amplitudes and phases were measured and compared with calculations for a range of nighttime ionospheric parameters. This avoided the problem of uncertainties in the transmitter powers. In this way the height, H', and the sharpness, β, when averaged over periods of several days, at least for the midlatitude *D* region near solar minimum, were found to be 85.1 ± 0.4 km and 0.63 ± 0.04 km^{-1}, respectively.

Citation: Thomson, N. R., M. A. Clilverd, and W. M. McRae (2007), Nighttime ionospheric *D* region parameters from VLF phase and amplitude, *J. Geophys. Res.*, *112*, A07304, doi:10.1029/2007JA012271.

1. Introduction

[2] Very low frequency (VLF) radio waves (~2–40 kHz) travel over the Earth's surface in the waveguide defined below by the oceans and the ground and above by the lowest level of the ionosphere known as the *D* region. During the middle of the day these VLF signals reflect mainly from heights in the range ~60–75 km, while at night, the electron densities are lower, and most of the reflection takes place in the range ~75–90 km. These (partial) reflections occur because the electron densities (and hence refractive indices) increase rapidly (in the space of a wavelength) with height in these ranges, typically from a few per cm^3 (or less) up to several hundred or more per cm^3. These electron densities are not readily measured by means other than VLF. Reflected amplitudes of higher frequency radio signals, such as those used in incoherent scatter radars, tend to be too small and so are masked by noise or interference. The air density at these heights is too high for satellites, causing too much drag. Rockets are expensive and transient; although some have given good results, there have generally been too few to cope with diurnal, seasonal, and latitudinal changes. In particular, flights at night have been especially few, with very tenuous results.

[3] Because VLF radio waves can penetrate some distance into seawater and because they can be readily detected after propagating for many thousands of kilometers, the world's great naval powers have built a number of powerful transmitters to communicate with their submarines. The phase and amplitude of the received signals provides a good measure, typically averaged over quite long distances, of the height and sharpness of the lower edge of the *D* region. The U. S. Naval Ocean Systems Center (NOSC), has developed computer programs (MODESRCH, MODEFNDR, Long Wave Propagation Capability (LWPC)) which take the input path parameters, calculate appropriate full-wave reflection coefficients for the waveguide boundaries, and search for those modal angles which give a phase change of 2π across the guide, taking into account the curvature of the Earth [e.g., *Morfitt and Shellman*, 1976; *Ferguson and Snyder*, 1990]. Further discussions of the NOSC waveguide programs and comparisons with experimental data can be found in the work of *Bickel et al.* [1970], *Morfitt* [1977], *Ferguson* [1980], *Morfitt et al.* [1981], *Pappert and Hitney* [1988], *Comité Consultatif International des Radio Communications* [1990], *Thomson* [1993], *Ferguson* [1995], *Cummer et al.* [1998], *McRae and Thomson* [2000, 2004], *Thomson and Clilverd* [2001], *Thomson et al.* [2005], and *Cheng et al.* [2006].

[4] The NOSC programs can take arbitrary electron density versus height profiles supplied by the user to describe the *D* region profile and thus the ceiling of the waveguide. However, from the point of view of accurately predicting (or explaining) VLF propagation parameters, this approach effectively involves too many variables to be manageable in our present state of knowledge of the *D* region.

[1] Physics Department, University of Otago, Dunedin, New Zealand.
[2] Physical Sciences Division, British Antarctic Survey (NERC), Cambridge, UK
[3] Gravitec Instruments Pty Ltd., c/o School of Physics (MO13), University of Western Australia, Perth, Australia.

0148-0227/07/2007JA012271

Table 1. Transmitter and Receiver Station Locations

Station	Latitude	Longitude
Dunedin	45.8°S	170.5°E
LaReunion	21.0°S	55.3°E
Argentina	43.1°S	65.2°W
Cambridge	52.2°N	0.1°E
NAA	44.6°N	67.3°W
NAU	18.4°N	67.2°W
Stanford	37.4°N	122.2°W
NPM	21.4°N	158.2°W
JJI	32.1°N	130.9°E
Faraday	65.3°S	64.3°W
NSS	39.0°N	76.5°W
NDT	35.0°N	137.0°E

As previously [*Thomson*, 1993; *McRae and Thomson*, 2000], we will follow the work of the NOSC group by characterizing the *D* region with a Wait ionosphere defined by just two parameters, the "reflection height," H', in kilometers, and the exponential sharpness factor, β, in km^{-1} [*Wait and Spies*, 1964]; the studies referenced in the previous paragraph also found this to be a satisfactory simplification. The LWPC version used here did not include the effects of ions (typically at least ~60,000 times more massive than the electrons) because at the frequencies used here (~10–40 kHz), their effects would likely be appreciably smaller than the fairly small effects (~0.15 km in H' and ~0.01 km^{-1} in β) noted by *Cummer et al.* [1998] at their somewhat lower frequencies. However, our version of LWPC did include the modifications described by *McRae and Thomson* [2000] to assure that LWPC uses a full range of modes and electron densities (as does ModeFinder), in particular that the minimum electron density went down to 0.1 el cm^{-3}, since this was found to be potentially significant.

[5] Daytime propagation is particularly stable, resulting in quite well-defined values of height and sharpness characterizing the lower *D* region, thus enabling calculation of the received VLF amplitudes and phases [*Thomson*, 1993; *McRae and Thomson*, 2000]. VLF propagation at night is often significantly more variable than by day. This appears to be partly due to the reflecting region of the ionosphere being more variable and partly because the night ionosphere supports more modes in the Earth-ionosphere waveguide which reach the receiver with significant amplitudes, thus resulting in more complicated modal interference which, in turn, results in the received amplitudes and phases being more sensitive to ionospheric changes than they are by day. This makes it very desirable to take measurements over many nights to establish a reliable pattern of average behavior.

[6] The early measurements of VLF propagation under the night ionosphere used airborne receivers which took amplitude measurements over a few Mm of path length over several hours [e.g., *Bickel et al.* 1970; *Morfitt et al.*, 1981]. The advantage of this method was that it reasonably quickly gave observational snapshots of the modal (amplitude) interference pattern as a function of distance from the transmitter. Since these interference patterns are relatively sensitive to the ionospheric parameters they are useful for testing ionospheric models. The disadvantage is that the night ionosphere is fairly variable and so the modal interference features can vary not only from night to night but during the flight, and, presumably because flights are expensive, relatively little data is available for averaging.

[7] Measuring and averaging the amplitudes and phases of VLF signals with a variety of frequencies over a variety of mainly all-sea paths has been found effective in markedly improving the accuracy of modeling the daytime lower *D* region for VLF propagation prediction [*Thomson*, 1993; *McRae and Thomson*, 2000]. Here we use a similar technique, with multiple frequencies and a variety of long, nearly all-sea paths, to improve the modeling of the nighttime *D* region parameters, and hence nighttime VLF propagation prediction.

2. VLF Transmitters (Omega and MSK) and Paths

[8] Phase and amplitude recordings used for determining the *D* region nighttime parameters here included those from the nearly all-sea paths, Omega La Reunion to Dunedin, NZ (10.1 Mm), Omega Argentina to Dunedin (8.7 Mm) and Faraday, Antarctica (2.5 Mm), and Omega Australia to Dunedin (2.1 Mm). The Faraday measurements were made in 1993 and the Dunedin measurements were all made in the period 1995–1997 prior to Omega shut down on 30 September 1997. The recordings were generally made on five frequencies between 10.2 kHz and 13.6 kHz.

[9] Also used were phase and amplitude recordings from (200 baud, frequency stable) U. S. Navy communications transmitters on nearly all-sea paths, recorded during 2005. These included NAA (24.0 kHz, Cutler, Maine, USA) to Cambridge, UK (4.9 Mm), NAU (40.75 kHz, Puerto Rico) to Cambridge (6.9 Mm) and NPM (21.4 kHz, Hawaii), to Stanford, California (3.9 Mm).

[10] All the phase and amplitude recordings were made on AbsPAL receivers [*Thomson et al.*, 2005; *McRae and Thomson*, 2004, 2000, and references therein] except for Omega Argentina to Faraday where an OmniPAL receiver was used. In addition some amplitude only data for nearly all-sea paths recorded on SCODAR VLF receivers [*Thomson*, 1993] was also available: NSS (21.4 kHz, Annapolis, Maryland) to Cambridge, U. K. (5.8 Mm, 1991), NAU (28.5 kHz, Puerto Rico) to Cambridge (6.9 Mm, 1991), NPM (23.4 kHz) to Stanford (3.9 Mm, 1991), NDT (17.4 kHz, Yosami, Japan) to Stanford (8.5 Mm, 1991), JJI (22.2 kHz, Kyushu, Japan) to Stanford (9.2 Mm, 1998). The latitudes and longitudes of all these transmitter and receiver stations are given in Table 1.

[11] Many more phase and amplitude, or amplitude only, recordings were available. However, preliminary analysis showed that recordings made predominantly over land (typically over relatively short paths) did not seem to give consistent results for the ionospheric parameters. Surprisingly, this also proved to be the case for (long nearly all-sea) paths which crossed the equator. Although many such recordings were available, none were used in determining the nighttime ionospheric parameters here.

[12] Because daytime propagation is now fairly predictable, and certainly more so than nighttime propagation, it was decided to use the differences between day and night amplitudes and the differences between day and night

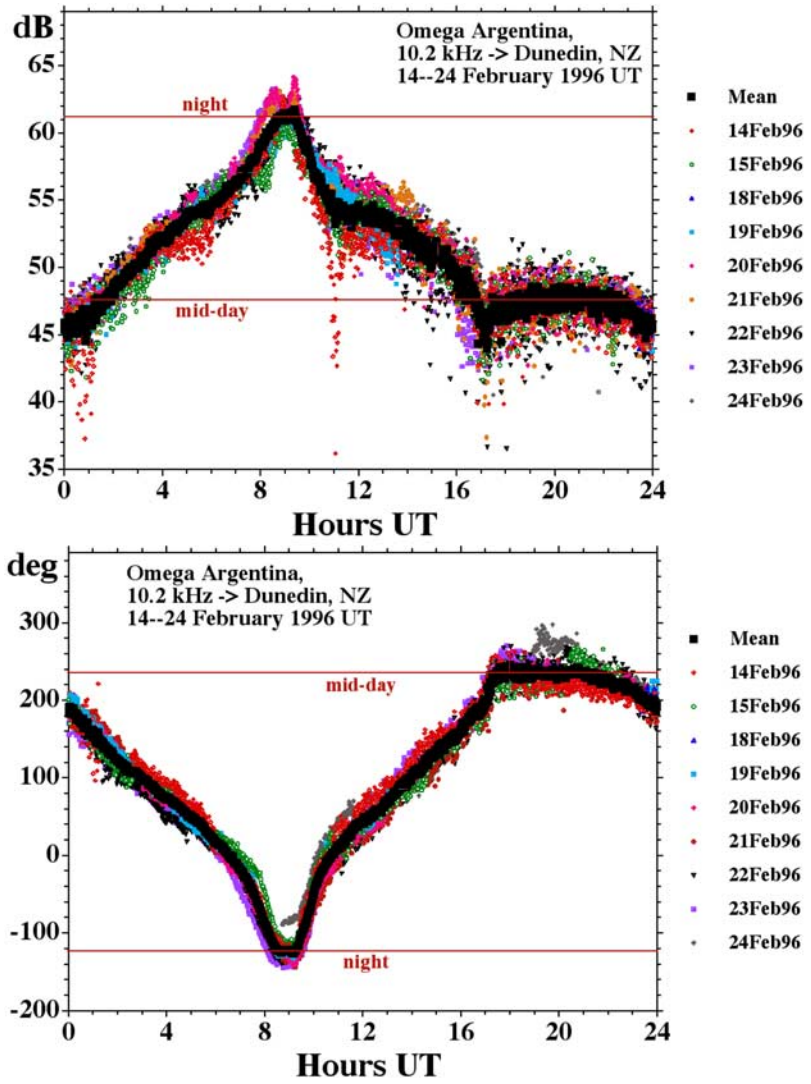

Figure 1. Amplitude and phase of 10.2 kHz from Omega Argentina, as measured at Dunedin, NZ, February 1996.

phases as the basis for determining the nighttime ionopheric parameters. This avoids the difficulty that the radiated powers of some of the communications transmitters are not well-known which would have made it difficult to be sure that the appropriate amplitude at the receiver was being calculated. Similarly, although the radiated powers of the Omega transmitters were well-known (at 10 kW), the absolute amplitudes at the receiver were normally not readily measured because of problems associated with the 10-s cycle of radiated frequencies. This use of day-night differences removes the need for any accurate knowledge of either the transmitter's radiated power or phase.

3. Ionospheric Parameters From Observations and Modeling

3.1. Omega Argentina Amplitude and Phase at Dunedin, NZ

[13] Figure 1 shows the observed amplitude and phase (relative to arbitrary base levels), as functions of hours UT, for the 10.2 kHz signals from Omega Argentina after propagating 8.7 Mm across the South Pacific Ocean to Dunedin, NZ, in the period 14–24 February 1996. The average midday (~2100 UT) and night (~0900 UT) amplitude and phase values from Figure 1, and from five other such similar (~7–9 day) recording periods during 1996, are plotted in Figures 2a and 2b as functions of their day number. Such phase plots, covering many months, are meaningful here because the Omega transmitters were maintained at constant phase (for navigational purposes) and the phases recorded by the AbsPAL receiver at Dunedin were referenced to GPS 1-s pulses. The horizontal lines in these phase and amplitude figures represent appropriate averages. For daytime, winter data have not been included in the averaging because the sun was not high enough in the sky for all the path to be fully day lit and readily modeled. The differences between these average lines in each figure thus give the observed differences in amplitude and phase between night and (equinoctial/summer) midday in each case.

[14] In Figures 2c and 2d, results for LWPC calculations for Omega Argentina on 10.2 kHz to Dunedin are shown for

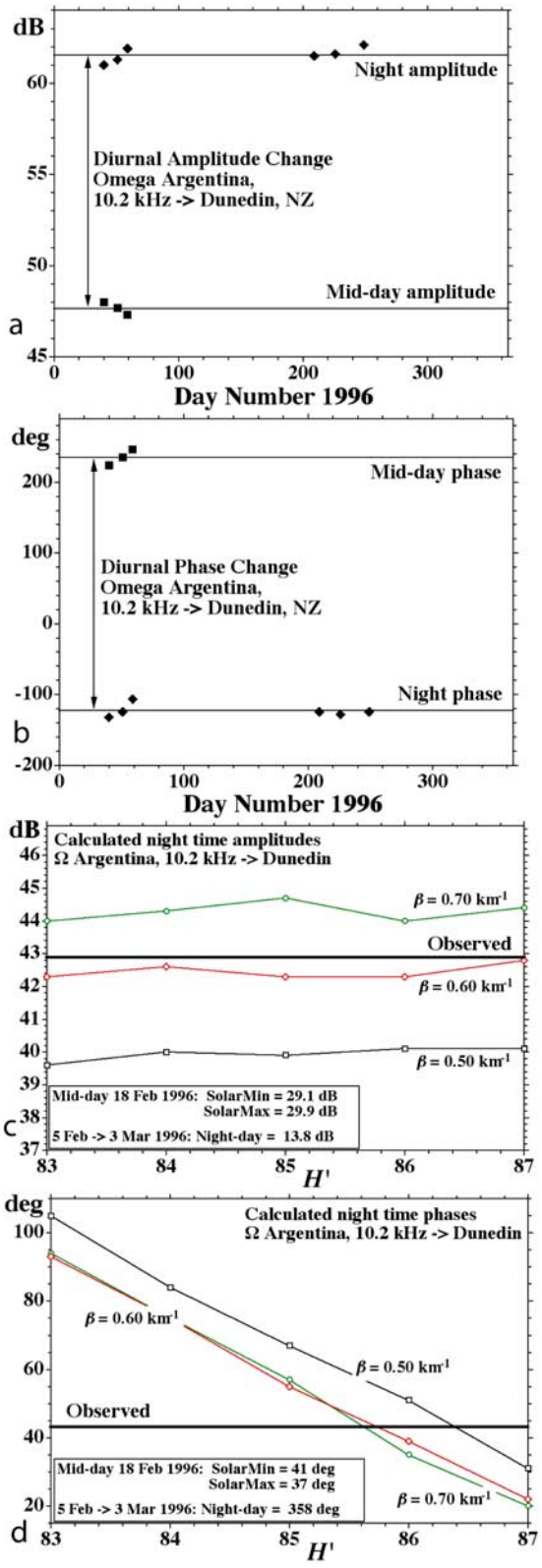

Figure 2. Omega Argentina, 10.2 kHz, measured at Dunedin showing (a,b) observed diurnal amplitude and phase changes and (c,d) comparisons of modeled and observed amplitudes and phases.

various values of H' (in the range 83–87 km) and β (in the range 0.50–0.70 km^{-1}), appropriate for nighttime propagation. The amplitudes are from LWPC's standard output in dB above 1 μV/m, assuming the normal Omega radiated power of 10 kW. The phases are also from LWPC's standard output in degrees (where the phase values increase when the ionospheric height lowers, e.g., during a solar flare, and decrease when the ionopheric height increases, e.g., in going from day to night). The text box, near the bottom of each of these figures, shows daytime amplitudes and phases calculated by LWPC for the transmitter and path near path midday for the equinoctial/summer date shown. The results of these LWPC calculations are shown for both solar minimum (using the daytime H' and β values determined by *McRae and Thomson* [2000]) and solar maximum (using the daytime H' and β values determined by *Thomson* [1993]). Also shown, in each text box, is the observed difference in phase or amplitude between day and night, as read from the lines in the top figures.

[15] These observed differences are then combined with the LWPC-calculated solar minimum values (since 1996 was solar minimum) in the text boxes to effectively give the observed nighttime amplitude and observed nighttime phase (in LWPC units) shown as thick bold horizontal straight lines in Figures 2c and 2d. It can thus be seen that H' = 85.7 km and β = 0.62 km^{-1} give good agreement between observations and modeling for phase and amplitude at 10.2 kHz for the 8.7 Mm, nearly all-sea path, from Omega Argentina to Dunedin, NZ.

[16] Figure 3 is for the same westward propagating Omega Argentina to Dunedin path as Figure 2, except for 13.6 kHz rather than 10.2 kHz. Figure 3 shows that H' = 85.4 km and β = 0.62 km^{-1} give the best fits for 13.6 kHz.

3.2. Omega La Reunion Amplitude and Phase at Dunedin, NZ

[17] Figures 4–6 show similar results to those of Figures 1–3 but for the eastward propagating 10.1 Mm path from Omega La Reunion across the Southern (Indian) Ocean to Dunedin, N.Z. As can be seen, Figure 5 shows the 13.6 kHz results giving H' = 85.1 km and β = 0.63 km^{-1}, while Figure 6 shows the 10.2 kHz results giving H' = 84.8 km and β = 0.61 km^{-1}. Because this path goes to quite high geomagnetic latitudes, reaching dip latitudes >~80° and L values >7, caution is needed in interpreting these results. The daytime ionospheric parameters used have not been tested at such high latitudes and may not be valid in these conditions. This issue is discussed further in section 4.4. All the other paths considered have dip angles below ~75° and L values below ~4.3, and so are essentially midlatitude in geomagnetic terms.

3.3. NAA (24.0 kHz), Maine, USA, to Cambridge, UK

[18] Figures 7 and 8 show results for U. S. Navy MSK transmitter NAA, Cutler, Maine, on 24.0 kHz recorded near Cambridge, U. K., after traveling about 4.9 Mm across the North Atlantic Ocean during the (northern) summer of 2005. Clearly, there is more variability at night (centered ~0200 UT) than by day (centered ~1400 UT). On this path, the received nighttime amplitudes and phases are somewhat sensitive to magnetic activity. Although this period (mid-June to mid-August) was not particularly magnetically

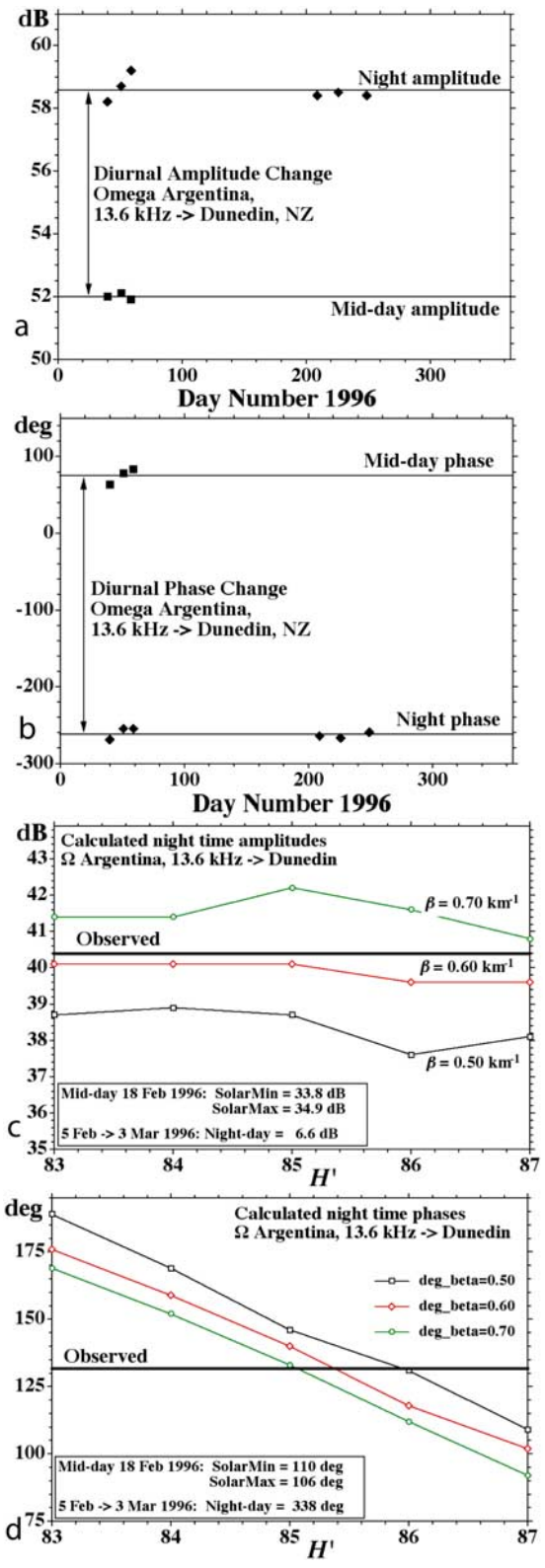

Figure 3. Omega Argentina, 13.6 kHz, measured at Dunedin showing (a,b) observed diurnal amplitude and phase changes and (c,d) comparisons of modeled and observed amplitudes and phases.

active, it was found desirable to identify the more active intervals by plotting the daily peak *Dst* index together with the measured daily amplitudes and phases (Figures 8a and 8b). Somewhat arbitrarily those periods with *Dst* below −40 were taken as magnetically active. For the two periods where *Dst* went below −60, a recovery period of 2 days was assumed, while for the less active period the recovery was assumed to be just 1 day. These active periods with their recovery times are shown shaded in Figures 8a and 8b.

[19] Only data observed during the unshaded (quiet) periods were used for comparing with LWPC calculations over a range of H' and β. Figures 8c and 8d show these comparisons, for NAA to Cambridge, in essentially the same way as was done in Figures 2, 3, 5, and 6 for the Omega paths to Dunedin. The results for the NAA path from LWPC daytime calculations for solar maximum and solar minimum are shown, as before, in the boxes near the bottom of each figure. Since 2005 is about 2/3 of the way from solar maximum to solar minimum, the LWPC daytime values actually used were taken in the same proportion. From Figure 8 it can be seen that the best fit is for H' = 84.7 km and $\beta = 0.64$ km^{-1}.

3.4. NAU (40.75 kHz), Puerto Rico, to Cambridge, U. K.

[20] NAU was recorded at Cambridge, U. K. (after traveling 6.9 Mm on a nearly all-sea path across the Atlantic) during the summer periods 9–16 July and 30 July to 15 Aug 2005. An example from the recordings is shown in Figures 9a and 9b. As can be seen, on some days, there is significant interference (affecting the amplitude much more than the phase) during the daytime at the Cambridge receiver (0700–1700 UT = 0800–1800 BST). However, the records are nonetheless quite useable for the present purpose. The 40.75 kHz of NAU was by far the highest frequency recorded and so its amplitude by day was especially low at the receiver but, even so, was quite unambiguous on a good number of days. The amplitudes in dB shown are relative to an arbitrary level and depend on (amongst other factors) the frequency response of the receivers and the exact orientation of the (loop) antennas. However, the day-night amplitude change (∼17.5 dB), and the day-night phase change are, of course, independent of all these factors.

[21] The interpretation of the day-night phase change in Figure 9b requires some care. When the received phase of a VLF transmitter can be tracked continuously over 24 hours with good signal to noise ratio, there may be no phase ambiguity; i.e., even the usual phase ambiguity of one cycle or 360° may not apply. This is commonly the case with the (relatively low frequency, on/off CW) Omega transmissions such as those received in Dunedin presented earlier. However, when there is modal interference or low signal to noise ratio, phase ambiguities of one cycle or 360° occur. In the case of MSK modulation (as now used by most VLF transmitters) the phase ambiguity is 180°.

[22] For NAA at Cambridge there were quite a number of days where it was clear from the records that the phase could be reasonably reliably tracked between day and night, with continuity preserved, and so the total day-night phase shift could be determined unambiguously. There were also quite a number of days when the phase could not be so

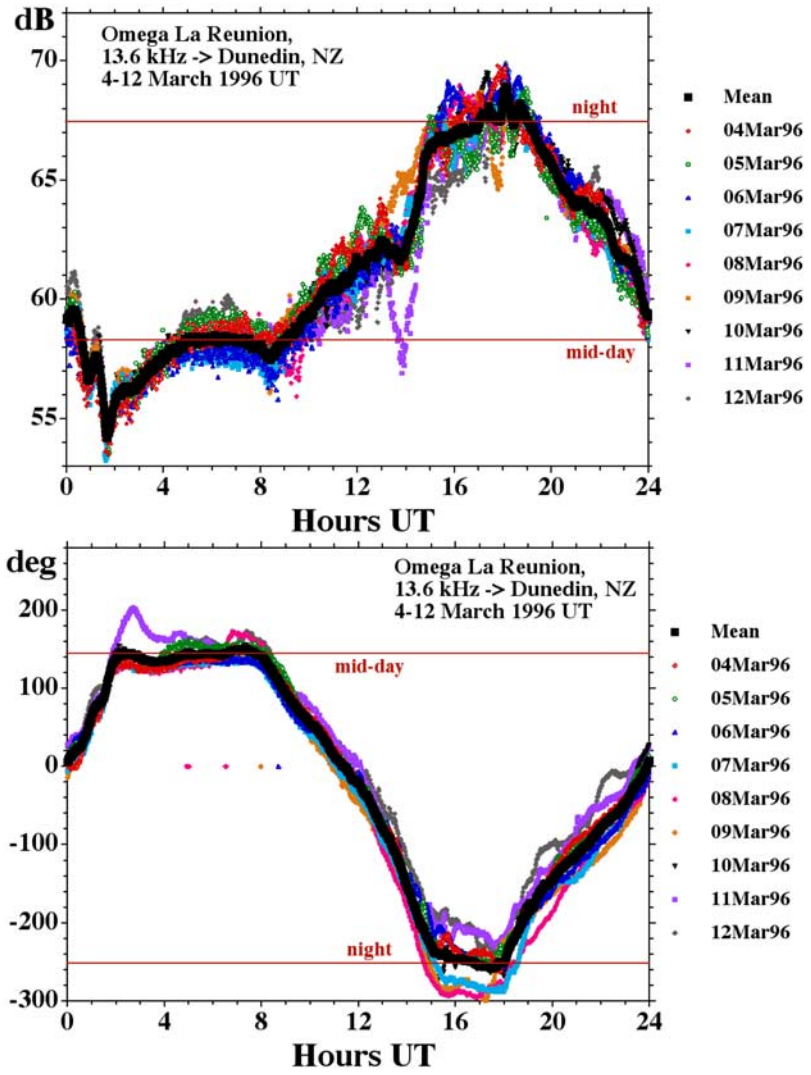

Figure 4. Amplitude and phase of 13.6 kHz signals from Omega La Reunion as measured at Dunedin, NZ.

reliably and continuously tracked, resulting in the day-night differences having ambiguities of a (small) integer multiple of 180°. However, the phase trackable days, being unambiguous, allowed the (multiple of) 180° ambiguity of many of the other days to be resolved.

[23] For NAU at Cambridge, the higher frequency (40.75 kHz), and the lower signal to noise ratio, made day-night continuous phase tracking (i.e., identifying cycle or half cycle slips) essentially impractical. Hence the day-night phase difference for NAU at Cambridge has half cycle (180°) ambiguities. Thus the "Observed" line shown in Figure 9d could equally be at 235° as shown or at 235° + 180° or 235° − 180°, etc. The line was placed at 235° because this gave values for H' similar to those found from the other paths; placing the "Observed" line 180° above or 180° below seemed unlikely in comparison with the other paths and frequencies. As for NAA in 2005, the calculated daytime values of amplitude and phase were for about 2/3 of the way towards solar minimum from solar maximum. Using the same process as for the other transmitters and paths, it can be seen from Figure 9 that, for NAU at Cambridge, the best nighttime ionospheric fit is for H' = 84.9 km and β = 0.63 km^{-1}.

3.5. NPM (21.4 kHz), Hawaii, to Stanford, USA

[24] The amplitude and phase for the 3.9 Mm path from NPM, Hawaii (21.4 kHz), to Stanford, California, USA, were recorded for the period 28 May to 7 June 2005. The results are shown in Figures 10a and 10b except for the phases on 31 May and 1 June 2005 when a problem with the GPS antenna siting caused some difficulties with the phase measurements. In Figures 10c and 10d, as was done for the other VLF paths here, the experimentally determined nighttime amplitudes and phases for NPM at Stanford are compared with LWPC calculations of nighttime amplitudes and phases using a range of nighttime ionospheric parameters. As before, the "Observed" nighttime amplitudes and phases have been found by combining the experimentally determined day-night changes (Figures 10a and 10b and boxes in Figures 10c and 10d) with the calculated daytime values (boxes in Figures 10c and 10d). As for the other 2005 data, the calculated daytime amplitudes and phases

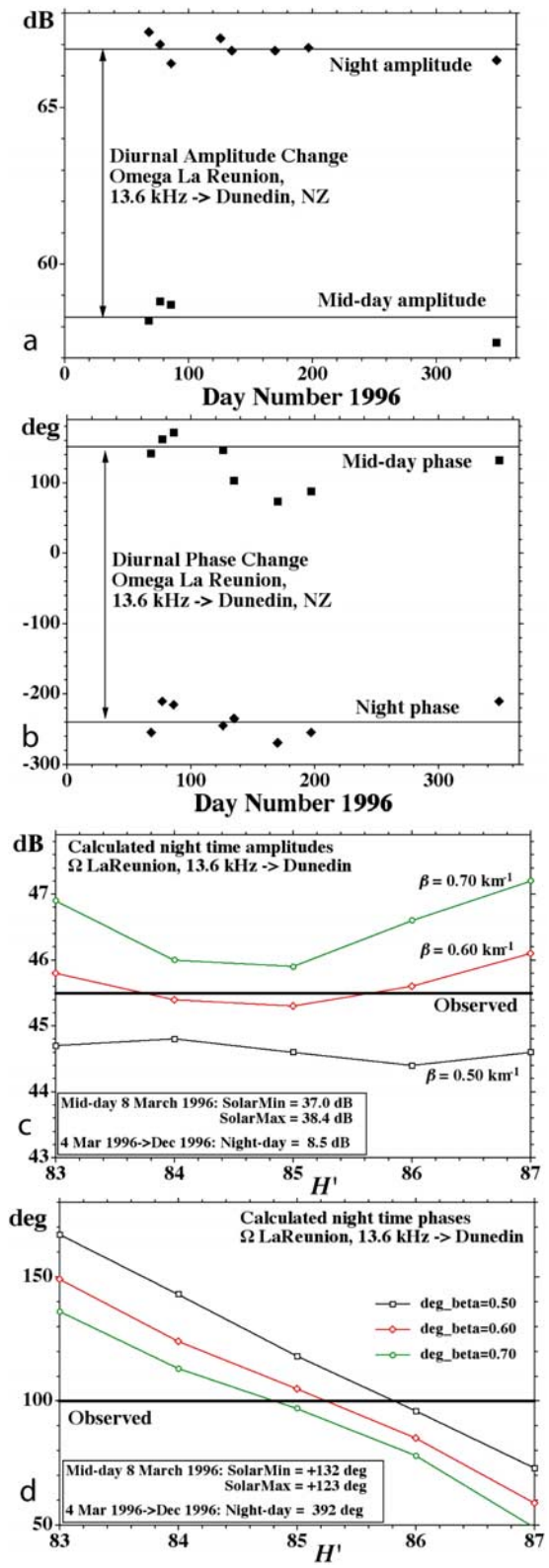

Figure 5. Omega La Reunion, 13.6 kHz, measured at Dunedin showing (a,b) observed diurnal amplitude and phase changes and (c,d) comparisons with modeled amplitudes and phases. See text for interpretation and assumptions.

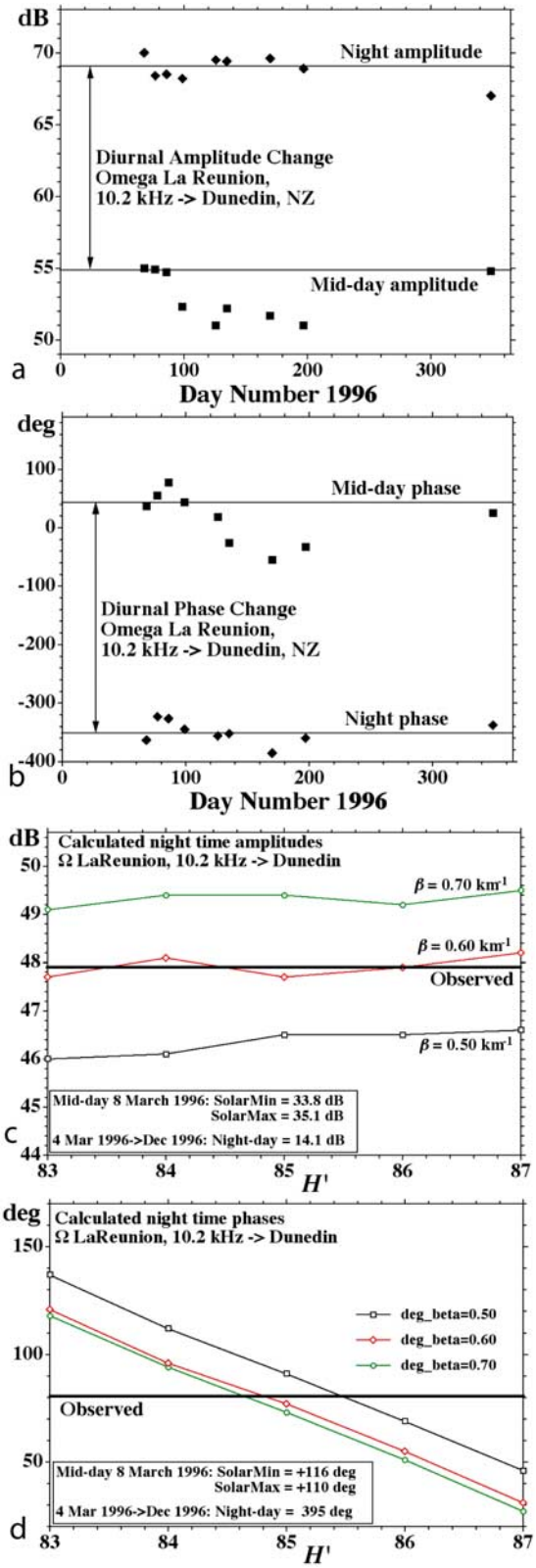

Figure 6. Omega La Reunion, 10.2 kHz, measured at Dunedin showing (a,b) observed diurnal amplitude and phase changes and (c,d) comparisons with modeled amplitudes and phases. See text for interpretation and assumptions.

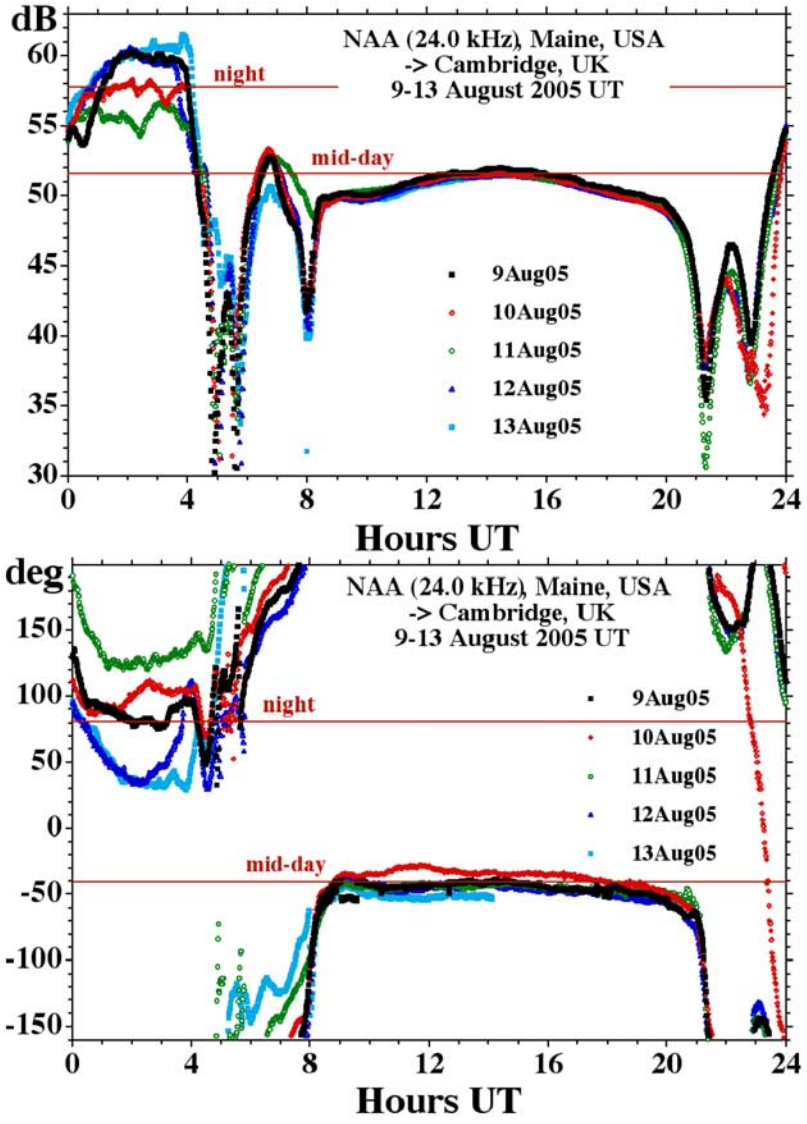

Figure 7. Amplitude and phase of NAA recorded at Cambridge, U. K.

used were interpolated for 2/3 of the way between solar maximum and solar minimum. As can be seen in Figures 10c and 10d, although the value of β is clearly not determined definitively, the NPM to Stanford results are none-the-less consistent with a nighttime ionosphere with $\beta = 0.60$–0.65 km^{-1} and $H' = 84.8$–85.0 km.

3.6. JJI (22.2 kHz), Kyushu, Japan, to Stanford, USA

[25] Amplitude only, in dB above an arbitrary reference level, of JJI (22.2 kHz), Kyushu, Japan, after propagating 9.2 Mm to Stanford, California, was recorded during 21–29 May 1998 using a SCODAR receiver [*Thomson*, 1985]. These amplitudes are shown in Figure 11a and, in Figure 11b, these observed amplitudes are compared, in the same way as for the previous paths, with those calculated from a range of *D* region ionospheric parameters. In Figure 11a it can be seen that one of the nighttime amplitudes (that for 29 May 1998) is much lower than the others. This may well have been due to a short sharp burst of magnetic activity on that day ($Kp = 7^-$ in one 3-hour period) so this day was excluded from the nighttime mean (the thick black line in Figure 11b). While Figure 11b provides little information on the height of the night *D* region, it clearly indicates that if H' is ~85.0 km (consistent with the previous results), then $\beta = 0.64$ km^{-1} gives the best fit; this is consistent with the results from the previous paths.

3.7. Other Midlatitude All-Sea Paths

[26] Recordings were available for a number of other midlatitude (nearly) all-sea paths. These included phase and amplitude for the 2.5 Mm path from Omega Argentina to Faraday and the 2.1 Mm path from Omega Australia to Dunedin. The day-to-day variations in amplitude and phase for these relatively short paths tended to be proportionately significantly greater than for the much longer paths, especially in amplitude. Comparison of the observed day-night changes in amplitude and phase with those calculated using $H' = 85$ km and $\beta = 0.63$ km^{-1} show satisfactory agreement but the proportionately higher errors mean that these short path comparisons do not contribute much to improving the

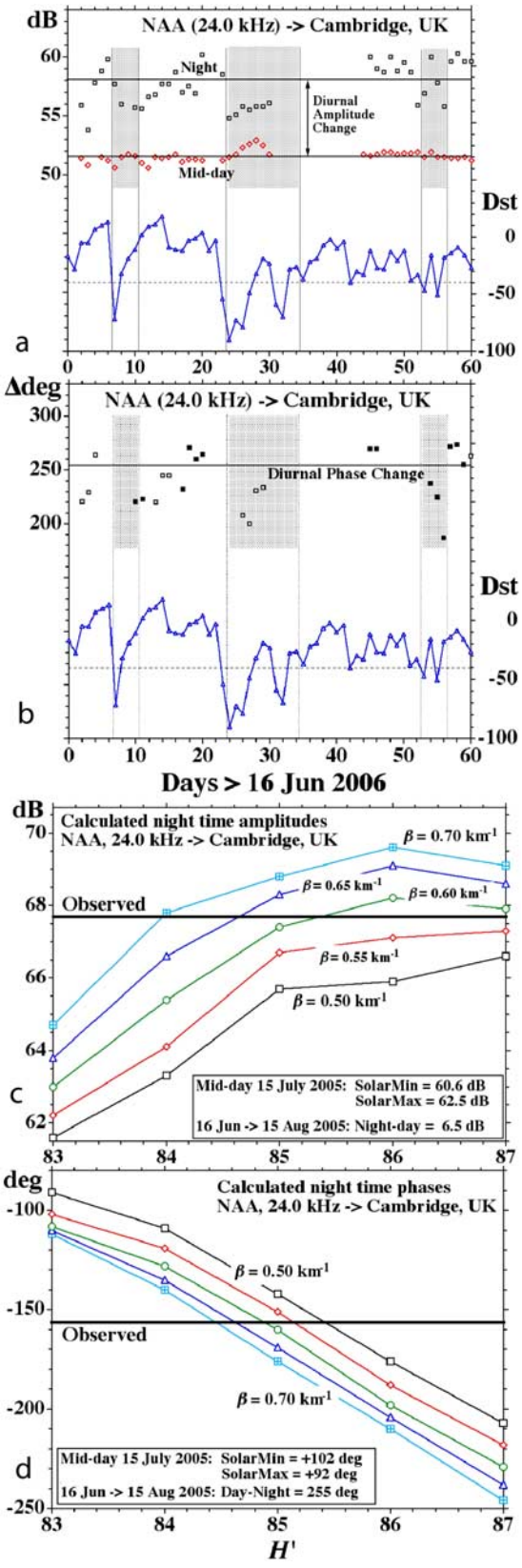

Figure 8. NAA, Maine, USA, 24.0 kHz, measured at Cambridge, UK showing (a,b) observed diurnal amplitude and phase changes and (c,d) comparisons of observations with modeled amplitudes and phases.

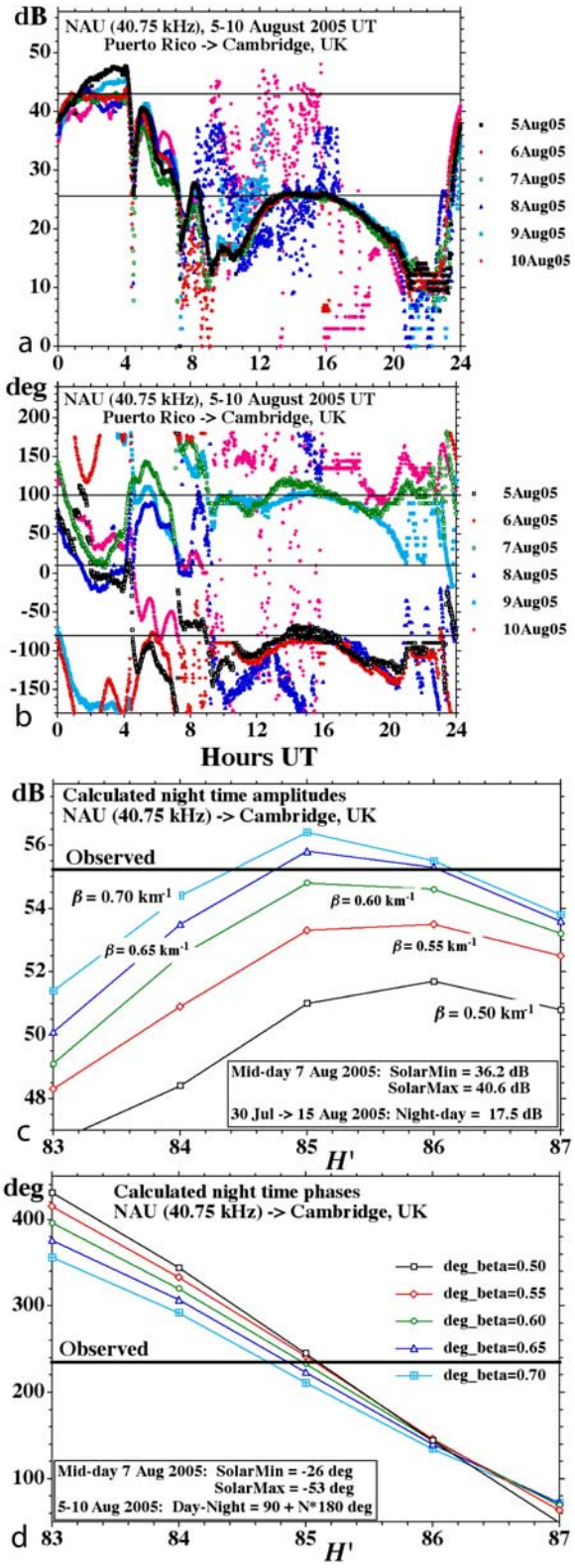

Figure 9. NAU, Puerto Rico, at Cambridge, UK showing (a,b) observed diurnal amplitude and phase changes and (c,d) comparison of observed and modeled amplitudes and phases.

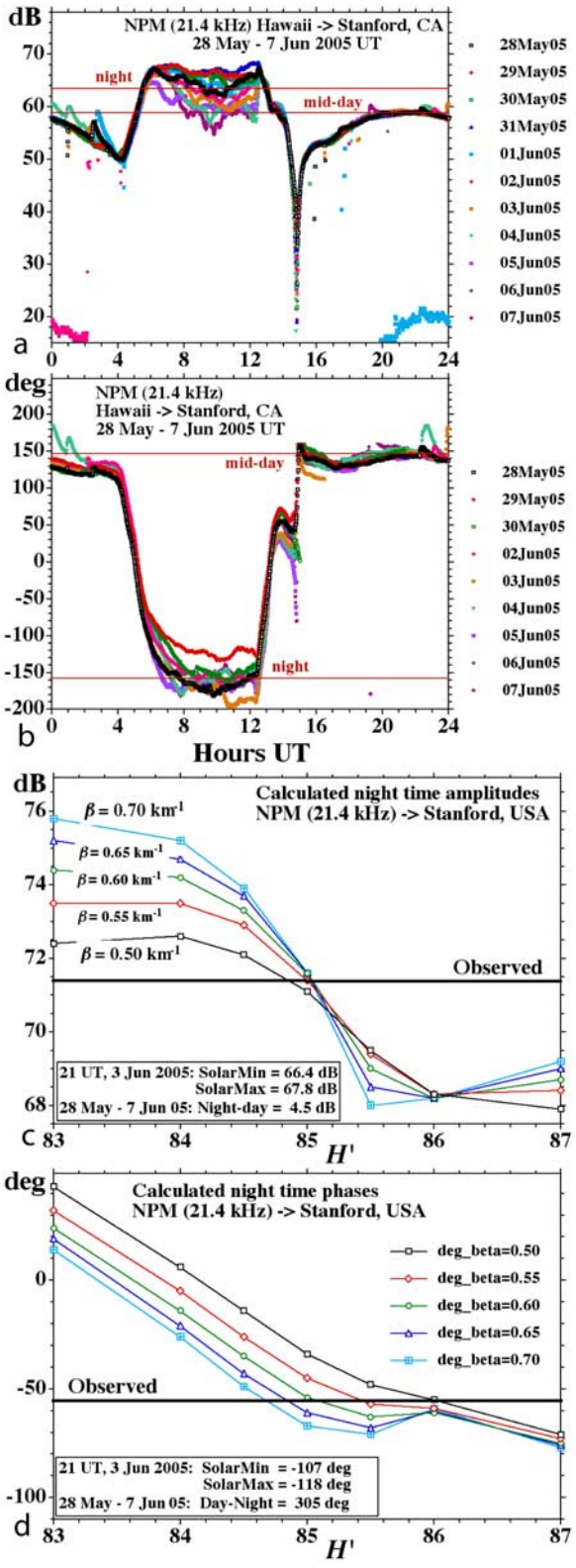

Figure 10. NPM, Hawaii, at Stanford, California showing (a,b) observed diurnal amplitude and phase changes and (c,d) comparison of observed and modeled amplitudes and phases.

determination of H' and β. This short path variability is consistent with the view that the night *D* region is significantly variable in time but that the greater spatial averaging occurring on long paths is likely smoothing these temporal variations along the long paths and thus giving rise to more stable results.

[27] Other (nearly) all-sea paths, but with only amplitude data available, included NAU (28.5 kHz, Puerto Rico), NSS (21.4 kHz, Maryland) and NAA to Cambridge, UK, and NPM (23.4 kHz, Hawaii) and NDT (17.4 kHz, Japan) to Stanford, all in the summer of 1991. These tended to give better agreement with $H' \sim 84$ km and $\beta \sim 0.60$ km^{-1} which could be because they were nearer solar maximum (compared with most of the rest of the observations being nearer solar minimum), but this was not conclusive. Thus all of the (nearly) all-sea, midlatitude paths investigated gave satisfactory agreement with H' in the range 84–85.5 km and $\beta \sim 0.60$–0.65 km^{-1}.

3.8. Paths Crossing the Equator

[28] Quite a number of (nearly) all-sea paths crossing the equator with good quality data were available, e.g., Omega Japan, Omega Hawaii, NPM (Hawaii), and NLK (Seattle) to Dunedin. However, the observations typically did not match well with calculations. For example, for Omega Japan on 10.2 kHz the observed amplitude at Dunedin (9.8 Mm away) was ~7 dB below what would have been expected from $H' = 85$ km and $\beta = 0.63$ km^{-1}; to get agreement a β value of <0.25 km^{-1} would be needed. This seems highly unrealistic. Previous work [*Thomson*, 1993; *McRae and Thomson*, 2004] found no such problems with daytime paths across the equator. These difficulties at night, for equatorial paths, remain under investigation.

3.9. Other Paths (With Significant Amounts of Land)

[29] Some short and medium length paths with significant amounts of land were briefly investigated. The medium length paths included NAA to Stanford (4.6 Mm) and NWC to Dunedin (5.7 Mm). The short paths involved mainly European transmitters received at Cambridge. Generally, there appeared to be some difficulties, possibly due to mode conversion involving ground irregularities and/or possible difficulties with LWPC's waveguide approach at short ranges. It was decided not to include an investigation of these paths for this report.

4. Discussion

4.1. Factors Determining *D* Region Electron Density

[30] Here we discuss some of the physical mechanisms that determine the nighttime *D* region electron density and make some comparisons with our experimental results. The principal source of ionization in the nighttime *D* region is usually assumed to be from neutral NO ionized (to $NO^+ + e^-$) by solar Lyman-α (121.6 nm) scattered (reradiated) by the neutral hydrogen in the Earth's geocorona [e.g., *Banks and Kockarts*, 1973]. As the Lyman-α penetrates the *E* and *D* regions, it is increasingly absorbed by O_2. An intensity of $\sim 2.5 \times 10^8$ photons/cm^2/s at an altitude of 85 km can be estimated from *Kazil et al.* [2003] for a typical nighttime solar zenith angle ~120°. Taking [NO] at this height as $\sim 1.5 \times 10^6$ cm^{-3} from Haloe [*Friedrich et al.*, 1998], and

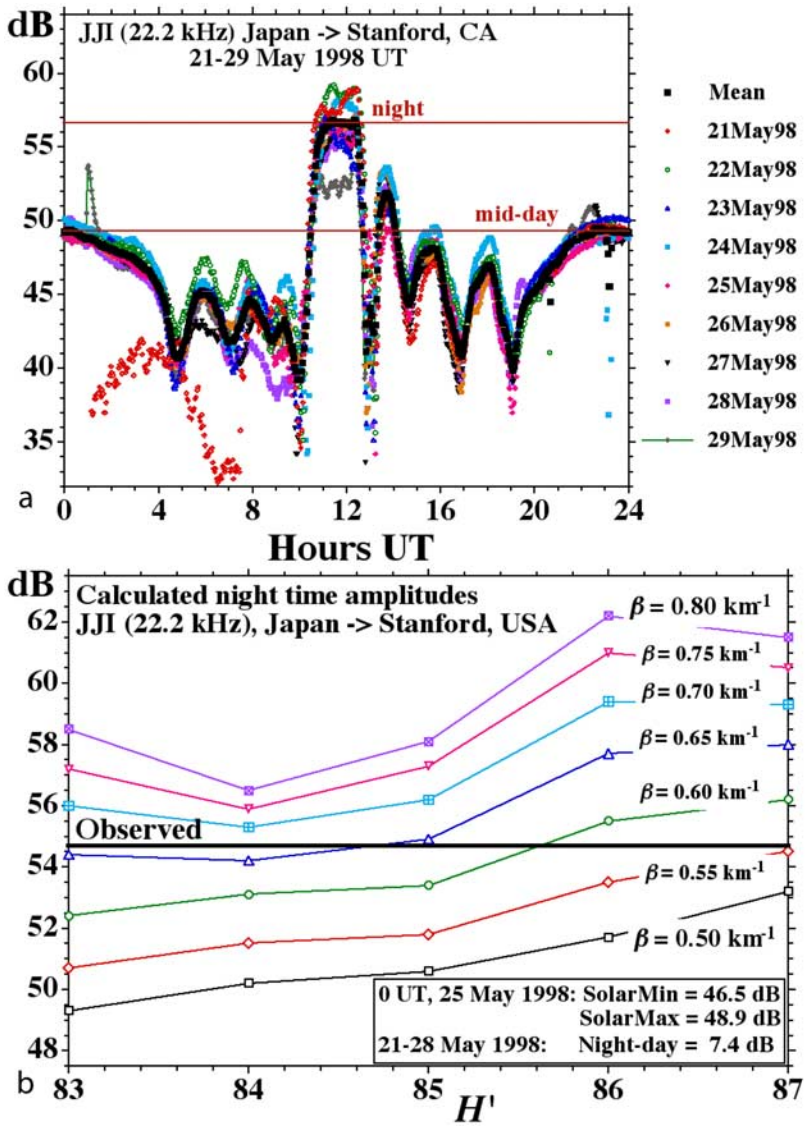

Figure 11. JJI, Kyushu, Japan recorded at Stanford, USA showing (a) observed amplitudes, with path in summer, and (b) comparison with modeled amplitudes.

the NO cross section as 2×10^{-18} cm^2 [*Banks and Kockarts*, 1973], the ionization rate is $\sim 7.5 \times 10^{-4}$ cm^{-3} s^{-1}. The recombination rate for $NO^+ + e^-$ is $\sim 4.5 \times 10^{-7}$ cm^3 s^{-1} at $\sim$200 K [*Sheehan and St-Maurice*, 2004]. Assuming equilibrium, and that these values represent the dominant process, they give $\sim$40 electrons/cm^3 at 85 km. From Figure 12, which shows the electron number density as a function of height for $H' = 85$ km and $\beta = 0.63$ km^{-1} (close to the values from the VLF observations here), it can be seen the agreement is good at 85 km. The electron densities (cm^{-3}) used by LWPC and shown in the figure are determined from $N(z) = 1.43 \times 10^7 \exp(-0.15H') \exp[(\beta - 0.15)(z - H')]$.

[31] However, considerable caution is needed since there are significant uncertainties particularly in [NO] and the scattered Lyman-α flux. Further, there is likely to be some additional recombination as discussed later in this subsection, and also there will be additional production due to galactic cosmic rays (GCR) for which the low-latitude ionization rate is 1.74×10^{-18} s^{-1} [*Heaps*, 1978]. From MSIS, the molecular number density at 85 km is $\sim 1.8 \times 10^{14}$ cm^{-3} which gives a GCR ionization rate of $\sim 3 \times 10^{-4}$ cm^{-3} s^{-1}, nearly half of the Lyman-α rate estimated above. Also, from *Heaps* [1978], by latitude 45°, this GCR rate increases by a factor of about 5 at solar minimum ($\sim$4 at solar maximum) and so GCR is clearly potentially an important source of ionization in the nighttime *D* region. The presence of two comparable sources of ionization will tend to somewhat smooth the variations of either: the effect of the nighttime solar zenith angle dependence of Lyman-α [e.g., *Kazil et al.*, 2003] is likely to be somewhat masked by the zenith angle independence of GCR, while the latitude dependence of GCR is likely to be somewhat smoothed by the relative latitude independence of the geocoronal Lyman-α.

[32] Going upward from 85 km, the Lyman-α flux increases (due to decreasing absorption by O_2) and the

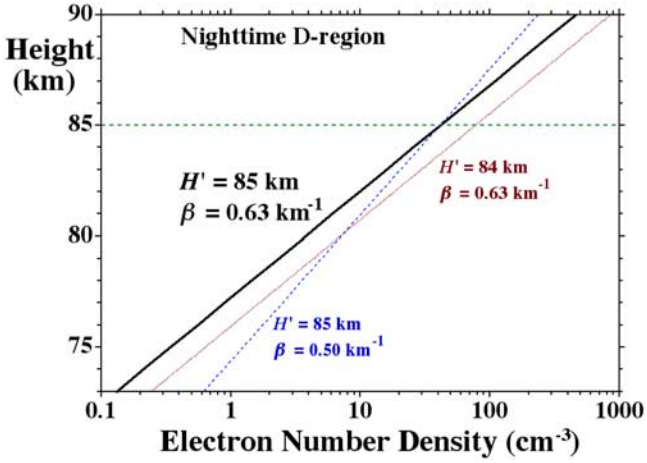

Figure 12. Electron density determined here (solid line). Similar profiles are shown for comparison (dotted lines).

NO density increases (since much of the NO diffuses down from the thermosphere above). These increases are, however, not enough to give the observed increases in electron density up to 90 km. These increases appear to be principally due to the presence of metal ions (Fe^+, Mg^+), probably of meteor origin, left over from daytime ionization. The metal ion recombination rate is very slow; so the metal ions and their electrons can survive the night at levels of $\sim 10^3$ el/cm^3 near 90 km [e.g., *Aikin and Goldberg*, 1973; *Swider*, 1984; *Kopp*, 1997].

[33] On going down below 85 km, a number of extra electron loss processes become very significant quite rapidly. One of these is the formation of water cluster ions, the rate of formation of which depends on the product of $[H_2O]$, which increases more rapidly than the neutral density [*Reid*, 1977] and [M] (where M = N_2 or O_2, etc.) which increases with the neutral density. The electrons then recombine more rapidly with these cluster ions than with NO^+. At least as significant, on going down in height, is the removal of electrons by attachment to O_2 to form (heavy) negative ions (O_2^- initially). The rate of this attachment reaction is proportional to $[O_2]^2$ [e.g., *Banks and Kockarts*, 1973] and is rapid even at 85 km. However, at 85 km the electrons are even more rapidly detached again by reacting with atomic oxygen, O. However, below 85 km, [O] decreases very rapidly with decreasing height and, of course, $[O_2]^2$ increases rapidly at the same time, with the result the electron density falls quite rapidly with decreasing height.

[34] All of these factors are reasonably consistent with the rapid change of electron density with height at night found here from the VLF radio measurements as shown in Figure 12. Unfortunately, the accuracies with which many of the parameters (densities and rates) are currently known probably do not yet justify a useful quantitative comparison.

4.2. Comparison With Rocket and Radar Electron Densities

[35] Very few in situ electron density measurements have been made in the night *D* region. The altitude is too low for satellites and the electron density has generally been too low for incoherent scatter radars. Only a very small number of nighttime rocket profiles measuring densities below $\sim$100 el/cm^3 exist for heights below $\sim$90 km. *Mechtly and Smith* [1968] and *Sechrist* [1968] reported two rocket probe measurements calibrated by Faraday rotation and differential absorption at Wallops Island (38°N) in the summer, just before sunrise, on 15 July 1964 at solar zenith angles of 108° and 96°. Their observed electron densities at 85 km were $\sim$70 and $\sim$40 cm^{-3}, respectively, very close to the 40 cm^{-3} found here. (The 40 cm^{-3} found nearer dawn than the 70 cm^{-3} earlier at 108° is likely to be indicative of the size of the effective error of these somewhat "spot" measurements.) At 80 km, the 108° measurement gave $\sim$3 cm^{-3} while at 96° $\sim$17 cm^{-3} was found. The first of these (i.e., well before dawn) is in good agreement with the densities found here at 80 km (Figure 12). At 90 km, the 1964 Wallops Island results gave $\sim$300 cm^{-3} compared with 500 cm^{-3} in Figure 12. However, many other rocket results, such as those discussed below have given $\sim$1000 cm^{-3}. Also by 90 km most of the VLF reflection has occurred; so the VLF sensitivity at 90 km is fairly low.

[36] *Smith* [1970] reported a series of nighttime rocket observations at Wallops Island in late winter on 22 February 1968. Four of the five profiles were taken in full night conditions (midnight to 0430 EST). At 85 km the electron densities averaged $\sim$30 cm^{-3} (ranging 10–40) while at 80 km the range was about 3–25 cm^{-3}. At 90 km the density was $\sim$1500 cm^{-3}. Because these results were in winter some may be a little high due to winter anomaly effects. *Mathews et al.* [1982] reported *D* region incoherent scatter electron densities on one night in August 1977. The densities at 85 km, well into the night, appeared to fluctuate around 40 cm^{-3}, similar to those found here, while at $\sim$90 km about 1000 cm^{-3} were found.

4.3. Comparison With Other VLF Measurements

[37] NOSC, under the auspices of which the VLF waveguide codes LWPC and ModeFinder were written, recommended (in LWPC) using $H' = 87$ km and $\beta = 0.50$ km^{-1} at night away from high latitudes. As discussed in the introduction, this was based on a relatively small number of aircraft flights, but using a good range of frequencies and nearly all-sea paths, during which continuous amplitude data was taken so that the details of the modal interference patterns were recorded and then later fitted to trial calculations using appropriate ranges of H' and β. *Morfitt et al.* [1981] summarize these results, including those of *Bickel et al.* [1970], with nighttime H' fits in the range 85.5–89 km and nighttime β fits in the range 0.3–0.7 km^{-1}. These best fit parameters tended to vary not only from path to path and flight to flight but also with frequency.

[38] *Cummer et al.* [1998] and *Cheng et al.* [2006] used frequencies in the range $\sim$2–20 kHz radiated by lightning, in well defined thunderstorm centers (to allow averaging), together with spectral fits with the LWPC propagation code to determine nighttime values for H' and β. The paths of *Cummer et al.* were $\sim$2 Mm to Stanford (in summer at 0415–0445 UT, 22 July 1996); the three paths from the east (over the Rockies) gave essentially $H' = 85.0$ km and $\beta = 0.50$ km^{-1} (after correcting for a $\sim$1.5 km ground altitude) while the path from the south (also over land) gave $H' = 86.1$ km and $\beta = 0.50$ km^{-1}. Cheng et al. used a similar procedure receiving VLF from lightning at Duke University

from storms ~700 km to the east (~60% sea, ~40% land) on 16 summer nights in 2004. They obtained H' and β values mainly in the ranges 83.6–85.6 km and 0.40–0.50 km^{-1}, respectively. These heights are generally in rather good agreement with the more global (and higher frequency) VLF results presented here. The values of β from the lightning are however quite a bit lower than the global, long-path, all-sea values presented here (~0.63 km^{-1}). This could be due to factors associated with the ground, such as lower conductivity than expected or scattering due to irregularities in conductivity in the ground or at the surface (mountains). There is also the possibility that LWPC, being based on discrete modes, does not perform so well at short distances, where modal approximations may not be fully adequate, or higher order modes may be missed.

4.4. Possible High-Latitude Effects

[39] In section 3.2 it was mentioned that the Omega La Reunion to Dunedin path has a significant part at high latitude (dip angle >80°, L >7) and that this might result in higher attenuation on the daytime path than would occur at lower latitudes. Indeed, if this could be the case, this might also perhaps be of some significance for the Omega Argentina path which goes to an even higher geographic latitude (but the dip <~75°, and L <~4.3 are lower). Omega Argentina was recorded on the same loop (directed ~geomagnetic east/west) as Omega Australia only 2.1 Mm away. The amplitude of the latter could be calculated with reasonable certainty and verified against some limited experimental observations. From the simultaneously recorded amplitudes on the same system, the received absolute amplitudes for Omega Argentina could thus be determined and these (at 10.2 kHz and 13.6 kHz) agreed very closely (<0.5 dB) with those found using the daytime LWPC calculations.

[40] Unfortunately, the position for Omega La Reunion to Dunedin is more difficult to assess. The other (north/south) loop was used and so Omega Australia could not be used for calibration. The much weaker Omega Hawaii was used instead with no observational confirmation. The results appeared to indicate that the daytime amplitudes of Omega La Reunion at Dunedin were ~2 dB below the LWPC modeled amplitudes. However, this is not at all conclusive. In particular, the receiving loop is on a slope tending downward to the northeast (toward Hawaii) and upward toward the southwest (toward La Reunion). Observations with a portable loop antenna in similar situations indicate that it would be quite possible for this lie of land to cause Hawaii to be ~1 dB more and La Reunion to be ~1 dB less. If this were the case, then the La Reunion results presented here would be fairly representing the true situation. If not, then the high-latitude La Reunion daytime path is degraded and so the corresponding La Reunion nighttime path is degraded too.

[41] So, in summary, if the La Reunion path is affected by high latitudes, it is unlikely that Omega Argentina path is too because the Argentina path has much lower L value, the lie of the land looks more symmetrical for Argentina and Australia, the Argentina path's daytime amplitudes are independently confirmed, and the dB change with beta is ~2 times greater for the Argentina path compared with the La Reunion path (see Figures 2, 3, 5, and 6). For the La Reunion path, the possible effect of the high latitudes, for both day and night, remains an open question.

5. Summary and Conclusions

[42] A series of global VLF phase and amplitude measurements has enabled improved parameters to be determined for the bottom edge of the (*D* region of the) Earth's nighttime ionosphere. These should prove useful for testing improved models of quiet time electron densities in this region and also for making improved quiet time VLF propagation predictions. Many interesting and significant perturbations are also observed in these regions: e.g., electron precipitation, sprites, gamma ray flares. These can hopefully be better studied from this improved quiet time base.

[43] The VLF observations were made mainly near solar minimum over midlatitude, nearly all-sea paths with lengths ~4–10 Mm in both northern and southern hemispheres and over the Atlantic, Pacific, and Southern (Indian) Oceans. The method for finding the quiet time night *D* region parameters involved measuring the changes in the observed phases, and the changes in the observed amplitudes, between (path) midday and night. Use was then made of well-established daytime *D* region ionospheric parameters to calculate the expected phases and amplitudes at the receivers for midday along the paths. These were then combined with the observed day-night changes to give the ''observed'' nighttime amplitudes and phases at the receivers. These ''observed'' nighttime values were then compared with nighttime propagation modeling using a range of possible nighttime *D* region ionospheric parameters. From these it was found that good agreement could be obtained if the lower edge of the (*D* region of the) night ionosphere is described by Wait parameters with heights in the range, $H' = 85.1 \pm 0.4$ km, and the sharpness, $\beta = 0.63 \pm 0.04$ km^{-1}, at least for the midlatitude *D* region near solar minimum, when averaged over several days. As discussed in section 3.7, rather tentatively, the corresponding parameters for near solar maximum may be $H' = 84$ km, $\beta = 0.60$ km^{-1}.

[44] **Acknowledgments.** We thank Tony Fraser-Smith for the very helpful use of his facilities at Stanford.

[45] Amitava Bhattacharjee thanks the reviewers for their assistance in evaluating this paper.

References

Aikin, A. C., and R. A. Goldberg (1973), Metallic ions in the equatorial ionosphere, *J. Geophys. Res.*, *78*(4), 734–745.

Banks, P. M., and G. Kockarts (1973), *Aeronomy*, Academic, New York.

Bickel, J. E., J. A. Ferguson, and G. V. Stanley (1970), Experimental observation of magnetic field effects on VLF propagation at night, *Radio Sci.*, *5*, 19–25.

Cheng, Z., S. A. Cummer, D. N. Baker, and S. G. Kanekal (2006), Nighttime *D* region electron density profiles and variabilities inferred from broadband measurements using VLF radio emissions from lightning, *J. Geophys. Res.*, *111*, A05302, doi:10.1029/2005JA011308.

Comité Consultatif International des Radio Communications (1990), Radio propagation and circuit performance at frequencies below about 30 kHz, *Doc. 6/1030-E (30 October 1989), Rep. 895-1*, 29 pp., XVII Plenary Assemb., Dusseldorf.

Cummer, S. A., U. S. Inan, and T. F. Bell (1998), Ionospheric *D* region remote sensing using VLF radio atmospherics, *Radio Sci.*, *33*(6), 1781–1792.

Ferguson, J. A. (1980), Ionospheric profiles for predicting nighttime VLF/LF propagation, *Naval Ocean Syst. Cent. Tech. Rep. NOSC/TR 530, NTIS Accession ADA085399*, Natl. Tech. Inf. Serv., Springfield, Va.

Ferguson, J. A. (1995), Ionospheric model validation at VLF and LF, *Radio Sci.*, *30*(3), 775–782.

Ferguson, J. A., and F. P. Snyder (1990), Computer programs for assessment of long wavelength radio communications, version 1.0: Full FORTRAN code user's guide, *Naval Ocean Syst. Cent. Tech. Doc. 1773*, *DTIC AD-B144 839*, Defense Tech. Inf. Cent., Alexandria, Va.

Friedrich, M., D. E. Siskind, and K. M. Torkar (1998), HALOE nitric oxide measurements in view of ionospheric data, *J. Atmos. Sol. Terr. Phys.*, *60*, 1445–1457.

Heaps, M. G. (1978), Parametrization of the cosmic ray ion-pair production rate above 18 km, *Planet. Space Sci.*, *26*, 513–517.

Kazil, J., E. Kopp, S. Chabrillat, and J. Bishop (2003), The University of Berne atmospheric ion model: Time-dependent modeling of the ions in the mesosphere and lower thermosphere, *J. Geophys. Res.*, *108*(D14), 4432, doi:10.1029/2002JD003024.

Kopp, E. (1997), On the abundance of metal ions in the lower thermosphere, *J. Geophys. Res.*, *102*(A5), 9667–9674.

Mathews, J. D., J. K. Breakall, and S. Ganguly (1982), The measurement of diurnal variations of electron concentration in the 60–100 km ionosphere at Arecibo, *J. Atmos. Terr. Phys.*, *44*(5), 441–448.

McRae, W. M., and N. R. Thomson (2000), VLF phase and amplitude: Daytime ionospheric parameters, *J. Atmos. Sol. Terr. Phys.*, *62*(7), 609–618.

McRae, W. M., and N. R. Thomson (2004), Solar flare induced ionospheric *D*-region enhancements from VLF phase and amplitude observations, *J. Atmos. Sol. Terr. Phys.*, *66*(1), 77–87.

Mechtly, E. A., and L. G. Smith (1968), Growth of the *D*-region at sunrise, *J. Atmos. Terr. Phys.*, *30*, 363–369.

Morfitt, D. G. (1977), Effective electron density distributions describing VLF/ELF propagation data, *Naval Ocean Syst. Cent. Tech. Rep. NOSC/TR 141, NTIS Accession ADA047508*, Natl. Tech. Inf. Serv., Springfield, Va.

Morfitt, D. G., and C. H. Shellman (1976), MODESRCH, an improved computer program for obtaining ELF/VLF/LF mode constants in an Earth-Ionosphere Waveguide, *Naval Electr. Lab. Cent. Interim Rep. 77T, NTIS Accession ADA032573*, Natl. Tech. Inf. Serv., Springfield, Va.

Morfitt, D. G., J. A. Ferguson, and F. P. Snyder (1981), Numerical modeling of the propagation medium at ELF/VLF/LF, *AGARD Conf. Proc.*, *305*, 1–14.

Pappert, R. A., and L. R. Hitney (1988), Empirical modeling of nighttime easterly and westerly VLF propagation in the Earth-ionosphere waveguide, *Radio Sci.*, *23*, 599–611.

Reid, G. C. (1977), The production of water-cluster positive ions in the quiet daytime *D* region, *Planet. Space Sci.*, *25*, 275–290.

Sechrist, C. F. (1968), Interpretation of pre-sunrise electron densities and negative ions in the *D*-region, *J. Atmos. Terr. Phys.*, *30*, 371–389.

Sheehan, C. H., and J.-P. St-Maurice (2004), Dissociative recombination of N_2^+, O_2^+, and NO^+: Rate coefficients for ground state and vibrationally excited ions, *J. Geophys. Res.*, *109*, A03302, doi:10.1029/2003JA010132.

Smith, L. G. (1970), A sequence of rocket observations of night-time sporadic-*E*, *J. Atmos. Terr. Phys.*, *32*, 1247–1257.

Swider, W. (1984), Ion and neutral concentrations of Mg and Fe near 92 km, *Planet. Space Sci.*, *32*, 307–312.

Thomson, N. R. (1985), Reflection of VLF radio waves from distant mountain ranges, *J. Atmos. Terr. Phys.*, *47*, 353–362.

Thomson, N. R. (1993), Experimental daytime VLF ionospheric parameters, *J. Atmos. Terr. Phys.*, *55*, 173–184.

Thomson, N. R., and M. A. Clilverd (2001), Solar flare induced ionospheric *D*-region enhancements from VLF amplitude observations, *J. Atmos. Sol. Terr. Phys.*, *63*(16), 1729–1737.

Thomson, N. R., C. J. Rodger, and M. A. Clilverd (2005), Large solar flares and their ionosperic *D* region enhancements, *J. Geophys. Res.*, *110*, A06306, doi:10.1029/2005JA011008.

Wait, J. R., and K. P. Spies (1964), Characteristics of the Earth-ionosphere waveguide for VLF radio waves, *Tech. Not. 300*, Natl. Bur. of Stand., Boulder, Colo.

M. A. Clilverd, Physical Sciences Division, British Antarctic Survey (NERC), High Cross, Madingley Road, Cambridge CB3 0ET, UK.

W. M. McRae, Gravitec Instruments Pty Ltd., c/o School of Physics (MO13), University of Western Australia, 35 Stirling Highway, Crawley, WA 6009, Australia.

N. R. Thomson, Physics Department, University of Otago, P. O. Box 56, Dunedin, 9054 New Zealand. (n_thomson@physics.otago.ac.nz)